ISSN 2394-3777 (Print)
ISSN 2394-3785 (Online)
Available online at www.ijartet.com
International Journal of Advanced Research Trends in Engineering and Technology (IJARTET)
Vol. 4, Issue 4, April 2017

Low Frequency Modular Multilevel Converter Topology for Improved Dynamic Performance of Variable-Speed AC Drives

G. S. R. Ajay Krishna[1], D. Krishna[2]
[1]M.Tech Student, Department of EEE, Anurag Group of institutions, Hyderabad, India.
[2]Asst. Professor, Department of EEE, Anurag Group of institutions, Hyderabad, India.

Abstract—This paper presents a control arrangement for the modular multilevel converter (MMC) to drive a variable-speed alternating current machine, mainly concentrating on upgrading dynamic fruition. In a manner, the energy balance in the MMC cell capacitors is prone to be unstable at start-up and low-frequency operations. Moreover, the MMC topology fundamentally requires advanced control methodology to modify imperativeness and smother the voltage pulsation of each cell capacitor. This paper proposes a control system for the healthy dynamic response of MMC even at zero frequency using leg offset voltage injection. The leg offset voltage for changing the arm energy is made by direct calculation but not the circulating current control controller. With the help of the exceedingly capable leg offset voltage from facilitate calculation the dynamic performance of a MMC at low speeds has clearly made progress. The ac machine has been driven from zero to maximum speed without enormous cell capacitor voltage ripples with help of this strategy. The proliferation and trial verify that relentless operation is guaranteed down to <2% of the rated speed under disturbance of 40% step load torque.

***Index Terms*— Dynamic performance, inner circulating current, Arm energy balancing, modular multilevel converter (MMC), motor drive.**

NOMENCLATURE

Superscript '*'	Reference value.
Superscript '~'	Low-frequency component.
Superscript 'Λ'	High-frequency component.
x -phase	Representation of one of the u, v, or w phases.
$v$xo	Leg offset voltage of x -phase leg.
$v$sn	Common mode voltage.
^{i}xo	Circulating current of x -phase leg.
ωs	Three-phase output frequency.
R	Resistance of arm inductor.
L	Inductance of arm inductor.
^{C}cell	Capacitance of dc capacitor in a sub module cell.
E_{xP}	Upper arm energy in x -phase leg.
E_{xN}	Lower arm energy in x -phase leg.
$v_{xPi}{}^{C}$	i th cell capacitor voltage in upper arm in x -phase.
$v_{xNi}{}^{C}$	i th cell capacitor voltage in lower arm in x -phase.

I. INTRODUCTION

A MODULAR multilevel converter (MMC) with concentrate on high-power medium voltage alternating current motor drives is conferred [1]–[10]. The usage of a MMC makes it possible to save gigantic parts in a medium-voltage motor drive application, for instance, a line-transformer, filter, and dc-link reactor. A differentiated and standard medium voltage source converter, the MMC has a specific structure made up of similar converter cells. Since it can give higher number of voltage level for medium voltage applications easily, the nature of the yield voltage waveform is better. Additionally, because of its structure it has purposes of enthusiasm, for instance, easy assembly and maintenance.

Figure. 1 demonstrates the circuit of a MMC. This topology should be controlled by additional control techniques. As demonstrated in Figure. 1, since the lower and upper arm currents flowing through cells, these arm currents cause pulsations of cell capacitor voltages. The pulsation of each cell's capacitor voltage is mainly affected by the output phase current and output frequency. Theoretically, the amount of the cell voltage fluctuation is proportional to amount of the output phase current and inversely proportional to working frequency [6]. Along these lines, remarkable effort is requested to drive the ac machine through MMC, which requires extensive starting torque and low-speed steady state operation. In late investigations of [7]–[9] and [16], the standards and calculations for alternating current motor drives with the MMC have been presented. In any case, they didn't address the real control procedures, for example, as, including standstill, changing output frequency and covering load torque disturbance.

The energy balancing control is one of the principle issues of a MMC framework. In various composed works [6]–

ISSN 2394-3777 (Print)
ISSN 2394-3785 (Online)
Available online at www.ijartet.com
International Journal of Advanced Research Trends in Engineering and Technology (IJARTET)
Vol. 4, Issue 4, April 2017

[10], the energy balancing controls of an MMC that utilizes modulation scheme and circulating current control have been presented. The leg offset voltage is utilized to manage the circulating current and has small impact on terminal voltages on ac and dc side. The regular control methods adjustment require the circulating current controller that delivers the leg offset voltage reference from the circulating current references with the help of PI controller or the proportional and resonant controller.

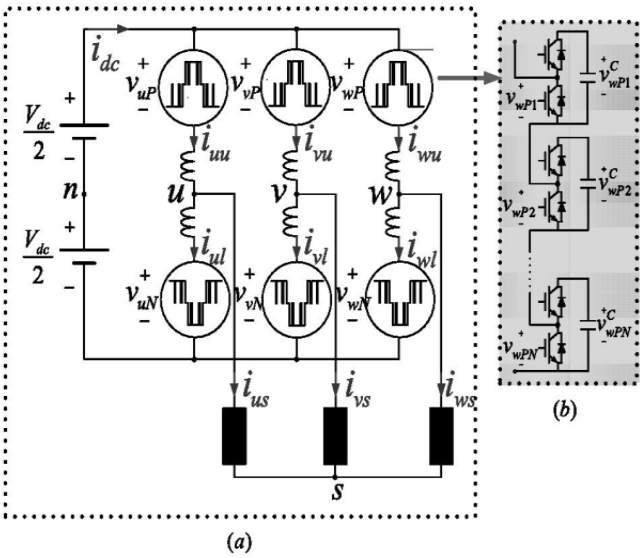

Fig.1. Circuit configuration of the MMC.

the execution of the circulating current controller has impact on the behavior of the balancing control. Therefore, to enhance the balancing performance by increasing bandwidth of the balancing controller, this paper proposes a balancing control method without the circulating current controller. In this way, in the view purpose of capacitor voltage adjusting, the offset leg voltage can be specifically gotten with no delay because of the circulating current controller. Along these lines, the data transfer capacity (bandwidth) of adjusting controller in light of the direct voltage injection technique can be enhanced more than that in view of the circulating current controller. Including, the dissimilarities between the cell voltages can be diminished quicker. Therefore, from the viewpoint of the control dynamics and control unpredictability, the proposed leg offset voltage injection strategy is preferable and more straightforward over the ordinary circulating current injection technique. Moreover, the leg offset voltage injection strategy with the high frequency can be enhanced more than that of current injection technique, due to the high frequency injection of the proposed technique. Consequently, attributable to the high-frequency injection with the strategy which is proposed, the variance of voltage in the cell capacitor can be within the limit compared with circulating current injection technique.

The target of this venture is to propose a control strategy for unrestricted frequency range operation along with zero speed for variable speed alternating current motor drive. The strategy which is proposed decreases the control execution reduction of the MMC when the load torque suddenly changes. The control method introduces two modes of operation namely: 1) a low-frequency mode for zero and low-speed operation and 2) a normal frequency mode from normal to higher speed operation. The procedure in the low-frequency mode abuses offset leg voltage and common mode voltage with the high-frequency component to smother the cell capacitor voltage swell. The square wave voltage is utilized as the leg balance voltage, which makes the circulating current peak is compressed when correlated with sinusoidal voltage waveform [7]. A switchover approach between two modes of operation is depicted to drive the alternating current machine in the overall operating speed region.

To confirm the capability of the proposed control scheme, a 12-kV 24-MVA MMC-based variable speed motor drive system was designed using the MATLAB software. The results of the simulation could offer the possibility and favorable position of the contrived technique for high-power nominal voltage drives with MMC. Also, tests for variable-speed alternating current motor drives by a 10-kVA model MMC mirroring blowers, pump drive framework, or fans were executed to check the feasibleness of the proposed balancing strategy. The analyses were directed for looking at elements of the sinusoidal and square wave leg offset voltage. The steady operation at 1 Hz, which is <2% of the evaluated speed, is appeared under an unexpected step load torque from 0% to 40% to exhibit the dynamic execution. The experiment shows that all control procedures involved were very used in the variable-speed alternating current motor drive framework with a load where the torque deviate in corresponding to the square of the speed, similar to pumps, fans, or blowers.

II. CONFIGURATION AND BASIC PRINCIPLE OF THE MMC

Fig. 1(a) shows the circuit configuration of the MMC. The three-phase MMC is composed of three legs and each leg has two arms and has an inductor in each arm. Each arm has *N*-identical half-bridge cells with cascade connection, and each cell consists of two switches and a dc capacitor. The cascaded cell modules in detail are shown in Fig. 1(b). In Fig. 1(a), i_{xl} and i_{xu} are the lower and upper arm currents, respectively, and i_{xs} is the

ISSN 2394-3777 (Print)
ISSN 2394-3785 (Online)
Available online at www.ijartet.com
International Journal of Advanced Research Trends in Engineering and Technology (IJARTET)
Vol. 4, Issue 4, April 2017

output phase current where x represents the u-, v -, or w-phase. The circulating current,i_{x0} and output phase current, i_{xs} are calculated from the upper and lower arm currents explained in (1) and (2). Therefore, the arm currents can be calculated as (3) and (4), according to the decoupled control scheme in [8] and [11]

$$i_{xu} = i_{xu} - i_{xl} \quad (1)$$

$$i_{x0} = \frac{i_{xu}+i_{xl}}{2} \quad (2)$$

$$i_{xu} = \frac{1}{2} i_{xs} + i_{x0} \quad (3)$$

$$i_{xl} = -\frac{1}{2} i_{xs} + i_{x0} \quad (4)$$

The leg offset voltage,v_{x0}, produces a circulating current defined as in (5), where R stand for the resistance and L stand for the inductance of an arm inductor when all the inductors in the arm of MMC are assumed to be identical. From the relationships of the voltages along the x -phase loop, the upper, and lower arm voltage references are denoted as (6) and (7), respectively, where v_{dc} is the dc-link voltage, and v_{xP} is the upper arm voltage and v_{xN} is the lower arm voltage. The common mode voltage, v_{sn} , is the difference in voltage between nodes s' and n', and v_{xs} is the phase voltage, which is $v_{xs} = v_m \cos(\omega_s t)$. A detailed mathematical description of the relationships in an MMC is given in [10]

$$v_{x0} = (R + L\frac{d}{dt}) i_{x0} \quad (5)$$

$$v^*_{xP} = \frac{V_{dc}}{2} - v^*_{xs} - v^*_{sn} - v^*_{x0} \quad (6)$$

$$v^*_{xN} = \frac{V_{dc}}{2} + v^*_{xs} + v^*_{sn} - v^*_{x0} \quad (7)$$

The instantaneous power of each arm in the *x* -phase can be deduced as (8) and (9). These two equations must be considered to understand of the proposed balancing control

$$P_{xp} = v^*_{xp} i_{xu} = \left(\frac{V_{dc}}{2} - v^*_{xs} - v^*_{sn} - v^*_{x0}\right)\left(\frac{1}{2} i_{xs} + i_{x0}\right) \quad (8)$$

$$P_{xN} = v^*_{xN} i_{xl} = \left(\frac{V_{dc}}{2} + v^*_{xs} + v^*_{sn} - v^*_{x0}\right)\left(-\frac{1}{2} i_{xs} + i_{x0}\right) \quad (9)$$

In addition, the upper arm energy can be calculated by (10) and lower arm energy can be calculated by (11). Each arm energy is the sum of the cell capacitor energies in the corresponding arm at *x* -phase leg

$$E_{xp} = \frac{1}{2} C_{cell} \sum_{i=1}^{N} (v^c_x p_i)^2 \quad (10)$$

$$E_{xN} = \frac{1}{2} C_{cell} \sum_{i=1}^{N} (v^c_x N_i)^2 \quad (11)$$

Furthermore, the 2nd order harmonic component can also be eliminated by the circulating current simultaneously to suppress the severe fluctuation of voltages in the cell capacitor. This control strategy is called as an averaging control.

III. PROPOSED BALANCING CONTROL SCHEME

A. Start-Up and Low Frequency Mode

The difference in power between the upper arm capacitor and lower arm capacitor, which is derived as (12) from (8) and (9), affects the cell capacitor voltage balance of the arms. The terms on the right-hand side in (12), $0.5V_{dc}i_{xs} - 2v^*_{xs}i_{x0}$ have considerable dc or very low-frequency components. Thus, when the output frequency is dc or very low, the voltage difference between the arms will diverge due to this low frequency term

$$P_{XP} - P_{xN} = 0.5V_{dc}i_{xs} - 2v^*_{xs}i_{x0} - 2v^*_{sn}i_{x0} - v^*_{x0}i_{xs}. \quad (12)$$

To balance the power difference between arms, a control strategy exploiting the common mode voltage, V_{sn} , was used in this project. The common mode voltage can be regarded as an additional degree of freedom for controllability since V_{sn} does not affect the line-to-line output voltage. The frequency of the common mode voltage is selected as a high frequency to minimize voltage fluctuations of the cell capacitor. In addition, since the circulating current,i_{x0} is also a controllable element that does not affect the output phase current, a high-frequency component can be superimposed on the circulating current. Hence, the third term on the right-hand side in (12), $2v^*_{sn}i_{x0}$can be used to balance the power of arms with the high frequency components in V_{sn} and i_{x0}. For convenience, the low- and high-frequency elements can be segregated from i_{x0} and V_{sn} as (13) and (14), where ~ and ^ refer to the low and high-frequency components, respectively

$$i_{x0} = \tilde{i}_{x0} + \hat{i}_{x0} \quad (13)$$

ISSN 2394-3777 (Print)
ISSN 2394-3785 (Online)
Available online at www.ijartet.com
International Journal of Advanced Research Trends in Engineering and Technology (IJARTET)
Vol. 4, Issue 4, April 2017

$$v_{sn} = \hat{v}_{sn} \qquad (14)$$

The power difference between the upper and lower arms can be rearranged from (12) to (14), and then, the low-frequency power component can be extracted as in (15). Here, the power difference is made zero by $\hat{v}_{sn}$

$$(P_{xP} - P_{xN})|_{\text{low freq.}} \approx 0.5V_{dc}i_{xs} - 2v_{xs}^{*}\tilde{i}_{xo} - 2\hat{v}_{sn}^{*}\hat{i}_{xo}^{*}\Big|_{\text{low freq.}} = 0. \qquad (15)$$

To nullify the low-frequency component as in (15), the low-frequency component of $2\hat{v}_{sn}^{*}\hat{i}_{xo}^{*}$ should be controlled. Thus, $\hat{v}_{sn}^{*}$ and $\hat{i}_{xo}^{*}$ should be regulated as the same high frequency, to make the power term of $2\hat{v}_{sn}^{*}\hat{i}_{xo}^{*}$ have dc or low frequency component.

In the case of the sinusoidal leg offset voltage injection method, $\hat{v}_{sn}^{*}$ and $\hat{v}_{xo}^{*}$ can be expressed as (16) and (17), and ωh refers to the angular speed of the high-frequency component, V_{sn} for the effective value of common mode voltage, and $\tilde{V}_{x0}$ for the magnitude of high-frequency leg offset voltage, which may have dc and several low-frequency components

$$\hat{v}_{sn}^{*} = \sqrt{2}V_{sn}\cos(\omega_h t) \qquad (16)$$

$$\hat{v}_{sn}^{*} = \tilde{V}_{x0}\cos(\omega_h t + \emptyset) \qquad (17)$$

The phase angle φ in (17) between the leg offset voltage and circulating current is derived from (18) to make the circulating current synchronize with the common mode voltage

$$\emptyset = arctan\left(\frac{\omega_h L}{R}\right) \qquad (18)$$

In general, ωhL is greater than R, because the frequency of injecting voltage is quite high. However, if the frequency is not high enough and the arm resistance cannot be ignored, the arm impedance parameters would need to be identified. For identification, at the system commissioning stage, the no interacting leg offset voltage can be injected into the arm, and the circulating current could be fed back as in (5). Consequently, the phase angle between the leg offset voltage and the circulating current in (18) can be obtained. Under the assumption of $R \ll \omega hL$, φ is approximately $\pi/2$. From (5), (16) and (17), the low-frequency component of the power associated with the common mode voltage and the circulating current can be derived as (19) using the leg offset voltage, where p represents a differential operator

$$\begin{aligned} 2\hat{v}_{sn}\hat{i}_{xo}\Big|_{\text{low freq.}} &\approx 2\hat{v}_{sn}\frac{\hat{v}_{xo}}{pL}\Big|_{\text{low freq.}} \\ &= \frac{2\sqrt{2}V_{sn}\tilde{V}_{xo}}{\omega_h L}\cos(\omega_h t)\sin\left(\omega_h t + \frac{\pi}{2}\right)\Big|_{\text{low freq.}} \\ &= \frac{2\sqrt{2}V_{sn}\tilde{V}_{xo}}{\omega_h L}\left(\frac{1}{2}\sin\left(\frac{\pi}{2}\right) + \frac{1}{2}\sin\left(2\omega_h t + \frac{\pi}{2}\right)\right)\Big|_{\text{low freq.}} \\ &= \frac{\sqrt{2}V_{sn}\tilde{V}_{xo}}{\omega_h L}. \end{aligned} \qquad (19)$$

And then, $2\hat{v}_{sn}^{*}\hat{i}_{xo}^{*}$ in (15) can be substituted with (19). The magnitude of high-frequency leg offset voltage, $\tilde{V}_{x0}$ can be calculated as

$$\frac{\sqrt{2}V_{sn}\tilde{V}_{xo}}{\omega_h L} \approx \frac{1}{2}V_{dc}i_{xs} - 2v_{xs}^{*}\tilde{i}_{xo}$$

$$\tilde{V}_{xo} \approx \frac{\omega_h L}{\sqrt{2}V_{sn}}\left(\frac{1}{2}V_{dc}i_{xs} - 2v_{xs}^{*}\tilde{i}_{xo}\right). \qquad (20)$$

In the case that the sinusoidal wave voltage is injected to both the common mode voltage (v_{sn}) and the leg offset voltage (v_{x0}), the balancing control strategy is shown as a block diagram in Fig. 2(a). E_{err} is the energy difference between the upper and lower arms as in (21). E_{err}^{*} is the reference of energy difference and should be set as null to keep the balance of the arm energies

$$E_{err} = E_{xp} - E_{xN} = \frac{1}{2}C_{cell}\{(v_x^c p_i)^2 - \sum_{i=1}^{N}(v_x^c N_i)^2\} \qquad (21)$$

P_{err}^{vff} in Fig. 2(a) can be derived as (22) by (20)

$$P_{err}^{vff} = \frac{1}{2}V_{dc}i_{xs} - 2v_{dc}^{*}\tilde{i}_{x0} \qquad (22)$$

In the case of the square leg offset voltage injection, on the other hand, the square wave voltage can be injected to both the common mode and the leg offset voltage as shown in Fig. 2(b). In this case, $\hat{v}_{sn}^{*}$ can be defined by (23) and f_h stands for the frequency of the injected high-frequency voltage

$$\hat{v}_{sn}^{*} = \begin{cases} -v_{sn} & \left(0 \le t < \frac{1}{2f_h}\right) \\ v_{sn} & \left(\frac{1}{2f_h} \le t < \frac{1}{f_h}\right) \end{cases} \qquad (23)$$

ISSN 2394-3777 (Print)
ISSN 2394-3785 (Online)
Available online at www.ijartet.com
International Journal of Advanced Research Trends in Engineering and Technology (IJARTET)
Vol. 4, Issue 4, April 2017

Under the assumption that the arm resistance, R, is dominant during each given quasisteady half period, $\frac{1}{2f_h}$,$\hat{v}^*_{xo}$ can be estimated as (24) from (5), (15), and (23)

$$\hat{v}^*_{xo} \approx \begin{cases} -\frac{R}{2V_{sn}}\left(\frac{1}{2}V_{dc}i_{xs} - 2v^*_{xs}\tilde{i}_{xo}\right) & \left(0 \le t < \frac{1}{2f_h}\right) \\ \frac{R}{2V_{sn}}\left(\frac{1}{2}V_{dc}i_{xs} - 2v^*_{xs}\tilde{i}_{xo}\right) & \left(\frac{1}{2f_h} \le t < \frac{1}{f_h}\right). \end{cases} \quad (24)$$

P^{vff}_{err} in Fig. 2(b) can also be derived from (22) using (24) similarly with the case of sinusoidal wave.

B. Normal Frequency Mode

Since the output frequency is high enough in the normal frequency mode, the voltage fluctuation of the cell capacitor is tolerable. In this mode, the circulating current is controlled to have only dc component to minimize the conduction loss caused by the additional circulating current. As the operation frequency increases, meanwhile, the boundary of the common mode voltage decreases. Hence, the common mode voltage availability is less for balancing control.

Practical MMC systems may have a built-in unbalance due to slight asymmetries in cells, structural errors, and other Issues. Therefore, in normal frequency mode it should be performed just to eliminate the present small dc unbalances. The balancing can be achieved using the circulating current as $2v^*_{xs}i_{x0}$ in (12). By adjusting the leg offset voltage for circulating current to have fundamental frequency component, this dc unbalance can be suppressed.

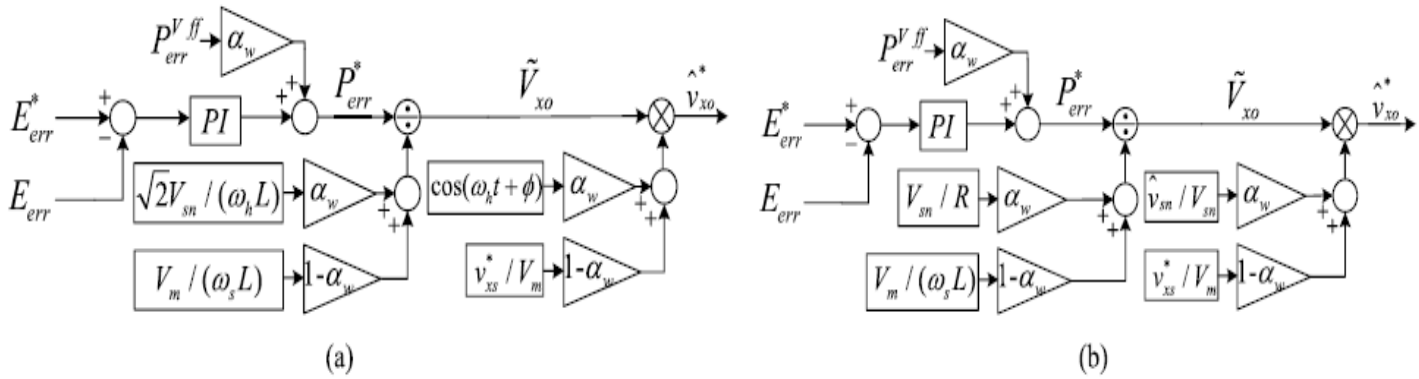

Fig.2. Proposed control scheme for variable-speed drives. (a) Sinusoidal wave voltage injection method. (b) Square wave voltage injection method. α_w is weighting factor for switchover, which is described in Section III-C.

C. Switchover Between Two Modes

As mentioned previously, as the high-frequency components of the common mode and leg offset voltage are only injected in low-operating frequency modes, the leg offset voltage reference changes with respect to the output frequency of MMC. A switchover tactic between the low- and high-frequency modes shown in Fig. 3 is devised by the weighting factor, α_w. In addition, this factor is applied to the switchover of the balancing control scheme shown in Fig. 2. In addition, the tactic would have the hysteresis band to prevent chattering in the vicinity of the switchover frequency, fcut.

IV. OVERALL CONTROL SCHEME FOR ENTIRE FREQUENCY OPERATION

Fig. 4 shows the overall controller for the entire frequency operation from standstill to normal frequency mode. First, the averaging controller regulates the leg power, which is the difference between output leg power and dc-link input power is calculated as (25) adding (8) and (9)

$$P_{xp} + P_{xN} \approx V_{dc}\tilde{I}_{x0} - 2v^*_{dc}\tilde{\imath}_{x0} - \hat{v}^*_{sn}i_{xs} \quad (25)$$

Because the low-frequency component of power in (25) should be nullified as in (26), the controller output has dc and second-order harmonic frequency components as described in (27)

ISSN 2394-3777 (Print)
ISSN 2394-3785 (Online)
Available online at www.ijartet.com
International Journal of Advanced Research Trends in Engineering and Technology (IJARTET)
Vol. 4, Issue 4, April 2017

$$P_{xp} + P_{xN} \approx V_{dc}\tilde{i}^{*}_{x0} - v^{*}_{xs}i_{xs} = 0 \quad (26)$$

$$\tilde{i}^{*}_{x0} = v^{*}_{xs}i_{xs}/V_{dc} \quad (27)$$

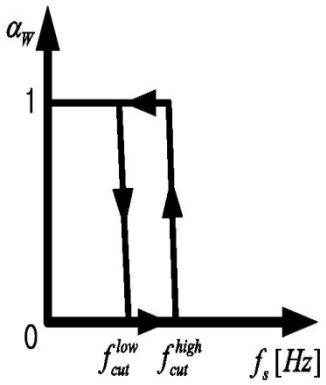

Fig. 3. Relationship between operating frequency and weighting factor.

E_{leg} is the energy of the leg and E_{leg} can be calculated as (28). E^{*}_{leg} is the reference energy of the leg as (29), where V^{*}_{c} is the reference value of cell capacitor voltage, V_{dc}/N

$$E_{leg} = E_{xp} + E_{xN} = \frac{1}{2}C_{cell}\left\{\sum_{i=1}^{N}(v^{c}_{x}p_i)^2 + \sum_{i=1}^{N}(v^{c}_{x}N_i)^2\right\} \quad (28)$$

$$E^{*}_{leg} = \frac{1}{2}\frac{C_{cell}}{2N}4N^2V^{*2}_{c} = NC_{cell}V^{*2}_{c} \quad (29)$$

The feed-forwarding power term, P^{vff}_{err}, can be derived as $v^{*}_{xs}i_{xs}$ from (27). Therefore, the PI controller can simply be adopted as the circulating current controller for the averaging

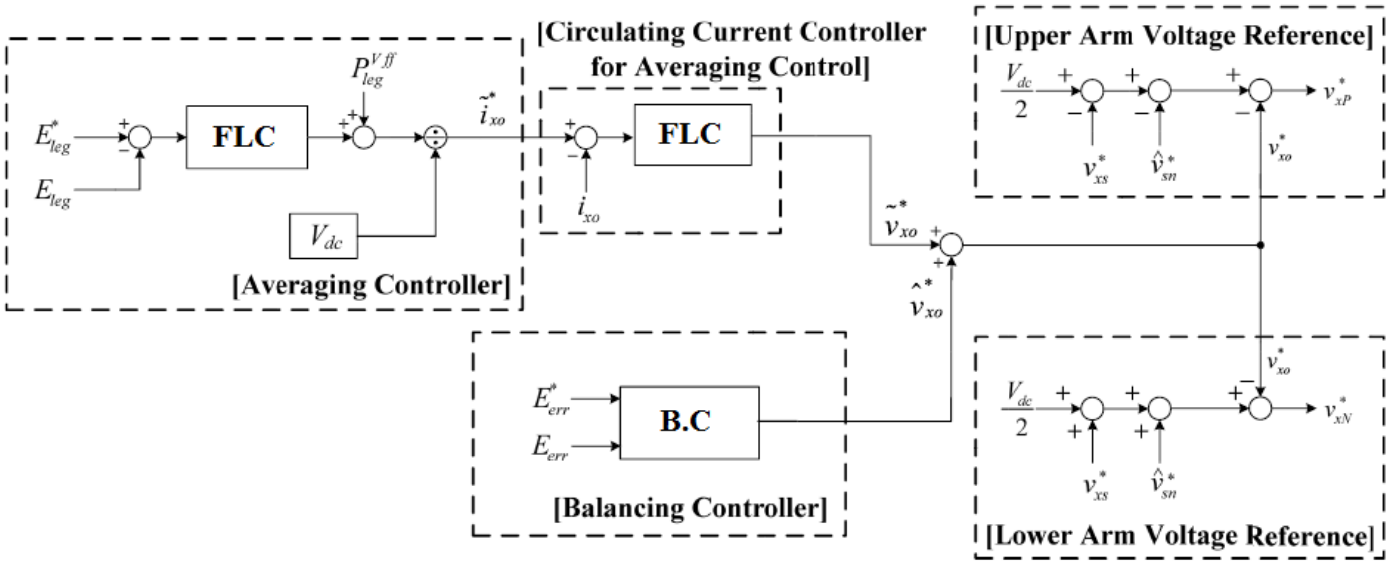

Fig.4. Proposed overall control scheme for variable-speed drives

control. The details about the averaging controller are described in [10].

In the interim, the balancing controller can be picked between two schemes in Fig. 2 that are in particular, the sinusoidal and the square wave voltage injections. As displayed in Fig. 4, the balancing controller specifically influences the leg offset voltage without the circulating current controller to wipe out the energy difference amongst upper and lower arms. By reason of this reality, the balancing controller has a more bandwidth, and can accomplish a superior transient response contrasted with the control arrangement in view of the inner circulating current regulation loop.

ISSN 2394-3777 (Print)
ISSN 2394-3785 (Online)
Available online at www.ijartet.com
International Journal of Advanced Research Trends in Engineering and Technology (IJARTET)
Vol. 4, Issue 4, April 2017

At last, the upper and lower arm voltage references are incorporated as (6) and (7), which are made out of v_{xs}^{*} from the yield of stage current controller, v_{x0}^{*} from the averaging and adjusting controller, and the infused normal mode voltage of $\hat{v}_{sn}^{*}$.

V. FUZZY LOGIC CONTROLLER

In FLC, essential control activity is dictated by an arrangement of etymological principles. These guidelines are controlled by the framework. Since the numerical factors are changed over into semantic factors, scientific displaying of the framework isn't required in FC. The FLC includes three sections: fuzzification, interference engine and defuzzification.

The FC is characterized as i. seven fuzzy sets for each input and output. ii. Triangular membership functions for simplicity. iii. Fuzzification using continuous universe of discourse. iv. Implication using Mamdani's, 'min' operator. v. Defuzzification using the height method.

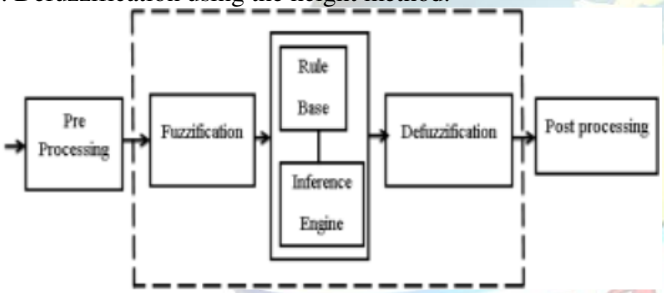

Fig.5 Fuzzy logic controller

Fuzzification: Membership function esteems are doled out to the etymological factors, using seven fuzzy subsets: NB (Negative Big), NM (Negative Medium), NS (Negative Small), ZE (Zero), PS (Positive Small), PM (Positive Medium), and PB (Positive Big). The partition of fuzzy subsets and the shape of membership CE(k) E(k) function adapt the shape up to appropriate system. The value of input error and change in error are normalized by an input scaling factor.

Table I FUZZY RULES

Change in error / Error	NB	NM	NS	ZE	PS	PM	PB
NB	NB	NB	NB	NB	NM	NS	ZE
NM	NB	NB	NB	NM	NS	ZE	PS
NS	NB	NB	NM	NS	ZE	PS	PM
ZE	NB	NM	NS	ZE	PS	PM	PB
PS	NM	NS	ZE	PS	PM	PB	PB
PM	NS	ZE	PS	PM	PB	PB	PB
PB	ZE	PS	PM	PB	PB	PB	PB

In this system the input scaling factor has been designed such that input values are between -1 and +1. The triangular shape of the membership function of this arrangement presumes that for any particular E(k) input there is only one dominant fuzzy subset. The input error for the FLC is given as

$$E(k) = \frac{P_{ph(k)} - P_{ph(k-1)}}{V_{ph(k)} - V_{ph(k-1)}} \qquad (14)$$

$$CE(k) = E(k) - E(k\text{-}1) \qquad (15)$$

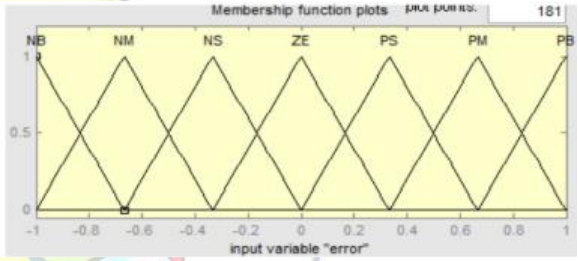

Fig.6 Membership functions

Inference Method: A few structure techniques, for example, Max– Min and Max-Dot have been proposed in the writing. In this paper Min strategy is utilized. The yield enrollment capacity of each lead is given by the base administrator and most extreme administrator. Table 1 indicates run base of the FLC.

Defuzzification: As a plant as a rule requires a non-fuzzy estimation of control, a defuzzification arrange is required. To process the yield of the FLC, "height" strategy is utilized and the FLC yield alters the control yield. Further, the yield of FLC controls the switch in the inverter. In UPQC, the dynamic power, responsive power, terminal voltage of the line and capacitor voltage are required to be kept up. Keeping in mind the end goal to control these parameters, they are detected and contrasted and the reference esteems. To accomplish this, the enrollment elements of FC are: blunder, change in mistake and yield. Christo Ananth et al.[5] presented a brief outline on Electronic Devices and Circuits which forms the basis of the Clampers and Diodes.
The set of FC rules are derived from

$$u=-[\alpha E + (1-\alpha)*C]$$

Where α is self-adjustable factor which can regulate the whole operation. E is the error of the system, C is the change in error and u is the control variable. A large value of error E indicates that given system is not in the balanced state. If the system is

ISSN 2394-3777 (Print)
ISSN 2394-3785 (Online)
Available online at www.ijartet.com
International Journal of Advanced Research Trends in Engineering and Technology (IJARTET)
Vol. 4, Issue 4, April 2017

unbalanced, the controller should enlarge its control variables to balance the system as early as possible set of FC rules is made using Fig.6 is given in Table 1.

VI. SIMULATION RESULTS

To check the sufficiency of the proposed control approach, an adaptable speed drive system based on 12-kV 24-MVA MMC has been implemented using the time-domain simulation program, MATLAB. The number of cells in each arm *N*, equals 20. Thus, the system with 120 cells was simulated. Each cell capacitor voltage is controlled as 600 V, and the cell is composed of the half-bridge inverter and the cell capacitance is 6000 μF. The nearest level modulation is applied to generate the arm voltage references and reduce the loss in switching action of MMC [15]. The cell voltage sorting algorithm is applied to the cell voltage balancing [14]. The parameters used in the simulations are listed in Table II.

TABLE II
CIRCUIT PARAMETERS OF THE SIMULATION

Description	Abbreviation	Value
Rated apparent power	S_{MMC}	24MVA
Rated line-to-line rms voltage	V_S	8.32kV
Rated line frequency	f_S	60Hz
DC-link voltage	V_{dc}	12kV
Cell capacitance	C_{cell}	6000μF
Arm inductance	L	4mH

TABLE III
PMSM SPECIFICATION OF THE SIMULATION

Description	Abbreviation	Value
Rated active power	P_{PMSM}	20MW
Rated line-to-line rms voltage	V_{rated}	8kV
Rated rotational speed	ω_{rm}^{rated}	360r/min
Pole pair number	pp	10

Simulink modeling diagrams:

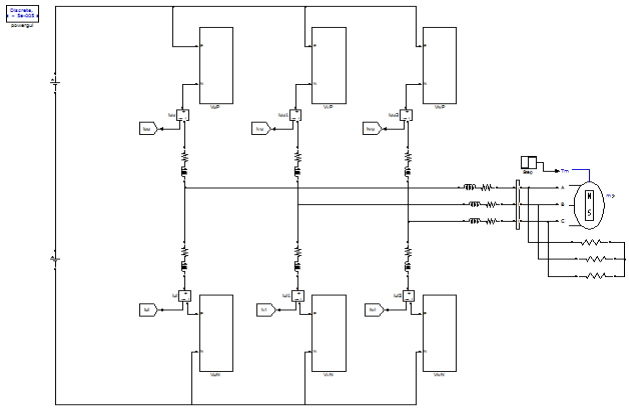

Fig.7 Block diagram of modular multilevel converter

ISSN 2394-3777 (Print)
ISSN 2394-3785 (Online)
Available online at www.ijartet.com
International Journal of Advanced Research Trends in Engineering and Technology (IJARTET)
Vol. 4, Issue 4, April 2017

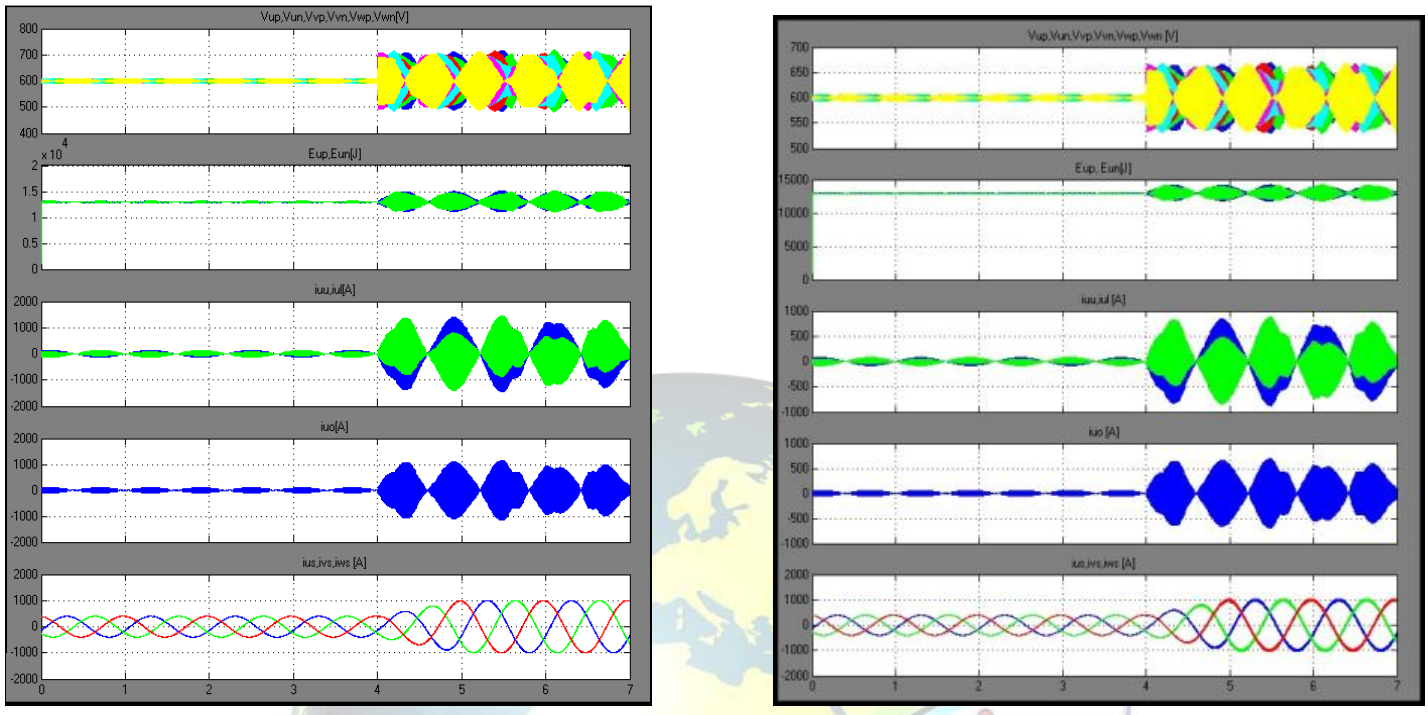

Fig. 8. Simulation waveform when applying the proposed leg offset voltage injection method with 6r/min speed and step load torque from 10% to 40% of the rated torque. (a) Sinusoidal waveform offset voltage injection (b) Square waveform offset voltage injection.

ISSN 2394-3777 (Print)
ISSN 2394-3785 (Online)
Available online at www.ijartet.com
International Journal of Advanced Research Trends in Engineering and Technology (IJARTET)
Vol. 4, Issue 4, April 2017

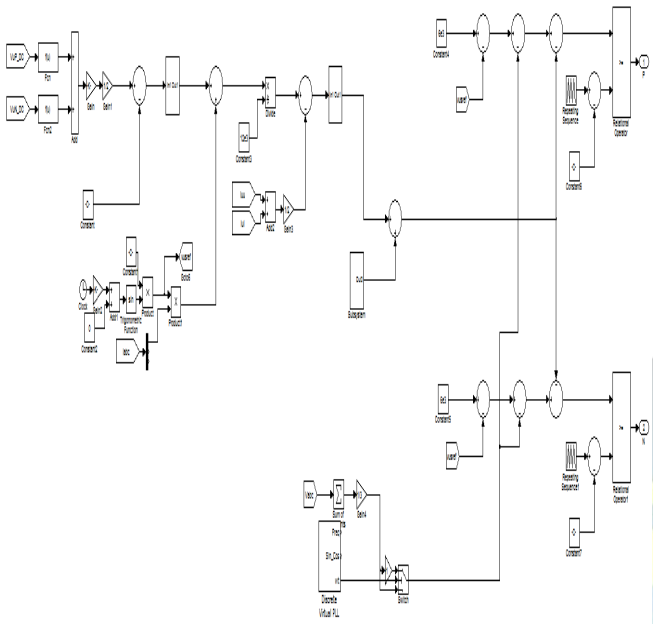

Fig.10 Overall control scheme

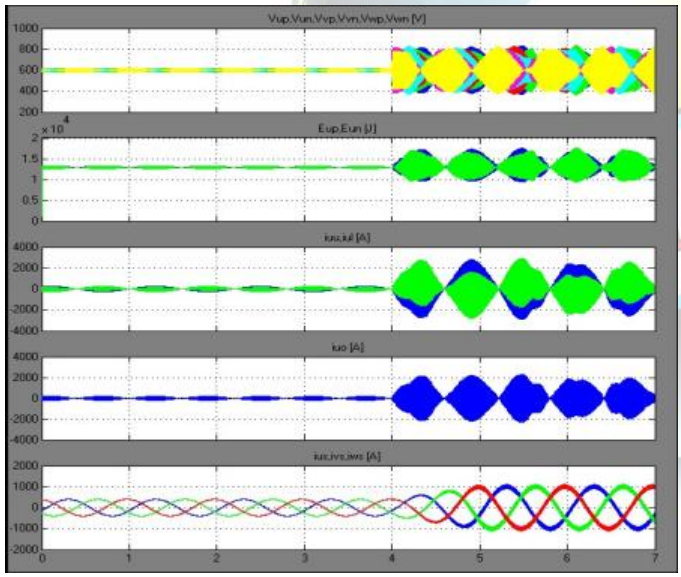

Fig 9. Simulation waveform when applying the conventional circulating current injection method with 6 r/min speed and step load torque from 10% to 36% of the rated torque

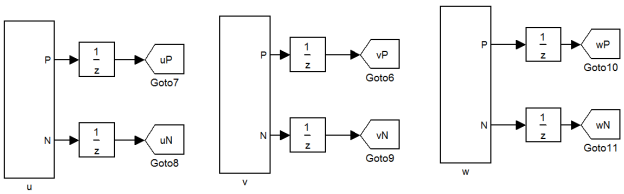

Fig.11 Block diagram of controller strategy

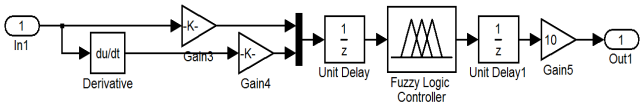

Fig.12 Fuzzy controller

It is assumed that the 21-level MMC system drives a 20 MW 20-pole permanent magnet synchronous machine (PMSM) with adjustable mechanical load. The PMSM parameters are summarized in Table III.

From the simulation results concocted technique can be connected to high-control medium voltage customizable drive framework in view of MMC. From the dynamic correlation between circling current infusion with the internal current circle and the proposed leg balance voltage infusion strategy, it can be presumed that the proposed technique may be a satisfactory answer for high-control medium voltage drives in view of MMC under necessities of extensive torque aggravation and unfaltering state operation down to a couple of percent of rated frequency.

Fig. 8 shows the low-frequency operation at 1 Hz (6 r/min, <2% of the rated frequency) with an ungracious step load torque from 50 kN · m (10%) to 200 kN · m (40%) at 4 s. Fig. 8(a) shows the simulation result of the sinusoidal wave leg offset voltage method, and Fig. 8(b) shows that of the square wave leg offset voltage method. The high recurrence (100 Hz) voltage is utilized to adjust the arm in low the recurrence mode in both sinusoidal and square wave cases. Before 4 s, the PMSM is controlled to be 6 r/min with 10% load torque. At the time point 4 s, the 40% load torque is suddenly connected to the PMSM. Notwithstanding the effect of step stack torque, MMC frameworks with both sinusoidal and square wave cases have effectively kept the steady operation. In the interim, looking at the waveforms between Fig. 8(a) and (b), the square waveform technique can spare the size of the flowing current. What's more, it has preferred adjusting capacity over the sinusoidal waveform strategy, from the perspective of the u-stage upper and lower cell capacitor voltage changes.

ISSN 2394-3777 (Print)
ISSN 2394-3785 (Online)
Available online at www.ijartet.com
International Journal of Advanced Research Trends in Engineering and Technology (IJARTET)
Vol. 4, Issue 4, April 2017

In the meantime, in Fig. 9, the simulation results with the ordinary circulating current implantation system in light of the internal current overseeing circle is showed up. Each working condition are indistinct to those in Fig. 8 beside the degree of the movement stack torque. For sensible examination between the customary current imbuement and proposed leg offset voltage mixture procedures, the information transmission for the modifying controller of the torque two strategies is set as the same, and the repeat of the implanted section was similarly set as the same, 100 Hz. The degree of the movement stack torque associated at the standard current imbuement procedure is 36% of the evaluated torque, which isn't precisely the proposed strategy test in Fig. 8. As showed up in Fig. 9, the system in perspective of the general procedure winds up obviously wobbly and backs off in a moment toward the end. After the sudden propel stack torque is associated at 4 s, the cell capacitor voltage changes are greater than the instabilities while using the leg adjust voltage implantation system in Fig. 8.

VII. Conclusion

In this paper, a control strategy for variable-speed ac motor drives based on MMC has been presented. To overcome the difficulties of the power balance between cells and arms of MMC over wide operation speed ranges, a direct leg offset voltage injection method has been devised. Using the professional postured technique, the swell voltage of every cell of MMC has been kept inside reasonable limits under the sudden utilization of 40% of evaluated stack torque at the to a great degree low recurrence, 1 Hz, which is <2% of appraised recurrence. In view of the reproduction and exploratory outcomes, it can be noticed that the control execution of the upper and lower arm vitality swell by the proposed leg counterbalance voltage infusion technique is superior to that by the customary coursing current infusion strategy with the inward circle. What's more, the variable speed air conditioning engine drive has been demonstrated to work in light of the switchover strategy by testing the general speed including zero speed.

REFERENCES

[1] A. Lesnicar and R. Marquardt, "An innovative modular multilevel converter topology suitable for a wide power range," in *Proc. IEEE Power Tech Conf.*, Bologna, Italy, Jun. 2003.

[2] Hiller, D. Krug, R. Sommer, and S. Rohner, "A new highly modular medium voltage converter topology for industrial drive applications," in *Proc. 13th Eur. Conf. Power Electron. Appl.*, Sep. 2009. pp. 1–10.

[3] G. P. Adam, O. Anaya-Lara, G. M. Burt, D. Telford, B. W. Williams, and J. R. McDonald, "Modular multilevel inverter: Pulse width modulation and capacitor balancing technique," *IET Power Electron.*, vol. 3, no. 5, pp. 702–715, Sep. 2010.

[4] H. M. Pirouz, M. T. Bina, and K. Kanzi, "A new approach to the modulation and DC-link balancing strategy of modular multilevel AC/AC converters," in *Proc. Int. Conf. PEDS*, 2005, vol. 2, pp. 1503–1507.

[5] Christo Ananth, W.Stalin Jacob, P.Jenifer Darling Rosita. "A Brief Outline On ELECTRONIC DEVICES & CIRCUITS.", ACES Publishers, Tirunelveli, India, ISBN: 978-81-910-747-7-2, Volume 3,April 2016, pp:1-300.

[6] M. Hagiwara, K. Nishimura, and H. Akagi, "A medium-voltage motor drive with a modular multilevel PWM inverter," *IEEE Trans. Power Electron.*, vol. 25, no. 7, pp. 1786–1799, Jul. 2010.

[7] M. Hagiwara, I. Hasegawa, and H. Akagi, "Start-up and low-speed operation of an electric motor driven by a modular multilevel cascade inverter," *IEEE Trans. Ind. Appl.*, vol. 49, no. 4, pp. 1556–1565, Jul./Aug. 2013.

[8] J. Kolb, F. Kammerer, and M. Braun, "Straight forward vector control of the modular multilevel converter for feeding three-phase machines over their complete frequency range," in *Proc. 37th Annu. Conf. IEEE Ind. Electron. Soc. IECON*, Nov. 2011, pp. 1596–1601.

[9] A. Antonopoulos, L. Angquist, S. Norrga, K. Ilves, and H.-P. Nee, "Modular multilevel converter AC motor drives with constant torque form zero to nominal speed," in *Proc. IEEE ECCE*, Sep. 2012, pp. 739–746.

[10] J.-J. Jung, H.-J. Lee, and S.-K. Sul, "Control of the modular multilevel converter for variable-speed drives," in *Proc. IEEE Int. Conf. PEDES*, Dec. 2012, pp. 1–6.

[11] L. Angquist, A. Antonopoulos, D. Siemaszko, K. Ilves, M. Vasiladiotis, and H.-P. Nee, "Inner control of modular multilevel converters-an approach using open-loop estimation of stored energy," in *Proc. IPEC*, Jun. 2010, pp. 1579–1585.

[12] T. Wang and Y. Zhu, "Analysis and comparison of multicarrier PWM schemes applied in H-bridge cascaded multi-level inverters," in *Proc. 5th ICIEA*, Jun. 2010, pp. 1379–1383.

[13] S. Rohner, S. Bernet, M. Hiller, and R. Sommer, "Modulation, losses, and semiconductor requirements of modular multilevel converters," *IEEE Trans. Ind. Electron.*, vol. 57, no. 8, pp. 2633–2642, Aug. 2010.

[14] X. Shi, Z. Wang, L. M. Tolbert, and F. Wang, "A comparison of phase disposition and phase shift PWM strategies for modular multilevel converters," in *Proc. IEEE ECCE*, Sep. 2013, pp. 4089–4096.

[15] M. Perez, J. Rodriguez, J. Pontt, and S. Kouro, "Power distribution in hybrid multi-cell converter with nearest level modulation," in *Proc. IEEE ISIE*, Jun. 2007, pp. 736–741.

ISSN 2394-3777 (Print)
ISSN 2394-3785 (Online)
Available online at www.ijartet.com
International Journal of Advanced Research Trends in Engineering and Technology (IJARTET)
Vol. 4, Issue 4, April 2017

[16] A. J. Korn, M. Winkelnkemper, and P. Steimer, "Low output frequency operation of the modular multi-level converter," in *Proc. IEEE ECCE*, Sep. 2010, pp. 3993–3997.

G. Ajay Krishna Completed B. TECH in Electrical & Electronics Engineering in 2015 from Sree Dattha College Of Engineering ,affiliated to Jawaharlal University, Hyderabad and Pursuing M.TECH form ANURAG Group of Institutions (Formerly known as CVSR College of Engineering(Autonomous)) Affiliated to JNTUH, Hyderabad, Telangana, India. Area of interest includes Power Electronics, electrical Machines and drives control.

Mr.D.Krishna, M.Tech (Ph.D) has a proven track record in Engineering and Technical Education. He obtained B.Tech in Electrical Engineering with first class and M.Tech in Control systems with first class and distinction. He is pursuing Ph.D. from reputed "Jawaharlal Nehru Technological University, Ananthapur. Area of interest is Power quality, Artificial intelligence in Power systems and Design and development of Fuzzy logic controller. Presently he is working as Assistant Professor of "Anurag Group of Intuitions" in Hyderabad, Telangana. He has a total experience of 12 years.